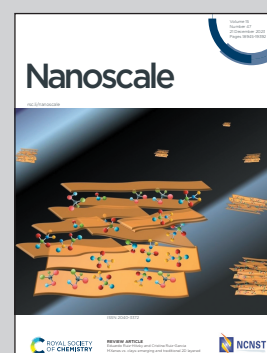# Liquid Marble

Review paper from Dr. Tenjimbayashi's Team at National Institute for Materials Science (NIMS), and Prof. Mouterde's Team at the University of Tokyo.

Liquid marbles: review of recent progress in physical properties, formation techniques, and lab-in-a-marble applications in microreactors and biosensors

This review summarises the fundamental properties of liquid marbles, the recent advances (mainly works published in 2020–2023) in the concept of liquid marbles, physical properties, formation methods, liquid marble-templated material design, and biochemical applications. Finally, the potential development and variations of liquid marbles are discussed.

As featured in:

Nanoscale

ROYAL SOCIETY OF CHEMISTRY

rsc.li/nanoscale

Nanoscale

Check for updates

Liquid marbles: review of recent progress in physical properties, formation techniques, and lab-in-a-marble applications in microreactors and biosensors

Mizuki Tenjimbayashi, [ID] *[a] Timothée Mouterde, [ID] *[b] Pritam Kumar Roy [ID] [b] and Koichiro Uto [ID] [c]

Liquid marbles (LMs) are nonsticking droplets whose surfaces are covered with low-wettability particles. Owing to their high mobility, shape reconfigurability, and widely accessible liquid/particle possibilities, the research on LMs has flourished since 2001. Their physical properties, fabrication mechanisms, and functionalisation capabilities indicate their potential for various applications. This review summarises the fundamental properties of LMs, the recent advances (mainly works published in 2020–2023) in the concept of LMs, physical properties, formation methods, LM-templated material design, and biochemical applications. Finally, the potential development and variations of LMs are discussed.

[a]*Research Center for Materials Nanoarchitectonics (MANA), National Institute for Materials Science (NIMS), 1-1 Namiki, Tsukuba, Ibaraki 305-0044, Japan. E-mail: TENJIMBAYASHI.Mizuki@nims.go.jp*

[b]*Department of Mechanical Engineering, The University of Tokyo, 7-3-1 Hongo, Bunkyo-ku, Tokyo 113-8656, Japan. E-mail: mouterde@g.ecc.u-tokyo.ac.jp*

[c]*Research Center for Macromolecules and Biomaterials, NIMS, 1-1 Namiki, Tsukuba, Ibaraki 305-0044, Japan*

1. Introduction

Transporting small amounts of liquids is essential in various fundamental industrial technologies that experience unwanted liquid adhesion. Nature offered an idea for effective liquid transportation. In 1992, Benton and Foster reported that some gall-forming aphids transport honeydew droplets without sticking by covering them with wax particles.[1] In 2001,

Mizuki Tenjimbayashi is an independent researcher at the Research Center for Materials Nanoarchitectonics (MANA), National Institute for Materials Science (NIMS). He received his Ph.D. from Keio University in 2017 and joined NIMS in 2018. He specializes in wetting dynamics and surface engineering to design functional materials interfaces with special wettability, such as superhydrophobic surfaces, liquid-infused surfaces, and liquid marbles. He is highly motivated to use his developments for practical application by joining industry–academia collaboration events.

Mizuki Tenjimbayashi

Timothée Mouterde graduated from École polytechnique and received his PhD from the Université Paris-Saclay. During his PhD supervised by David Quéré, he worked on antifogging surfaces and the dynamics of Leidenfrost and superhydrophobic drops. He then joined the group of Lydéric Bocquet, (ENS Paris) to study experimentally fluid transport inside angstrom-scale channels. In 2019, he moved to The University of Tokyo, in Takuro Ideguchi's laboratory, to develop new optical techniques for nanofluidics. In 2021, he started his research group within the Department of Mechanical Engineering of The University of Tokyo. His laboratory focuses on fluid/solid interactions from wetting phenomena to nanofluidics.

Timothée Mouterde

Aussillous and Quéré generalised the non-sticking property to water droplets by covering them with a hydrophobic powder and termed them liquid marbles (LMs).[2]

After two decades of research, LMs generally refer to liquids covered with low-wettability fine granular materials with non-sticking properties (Fig. 1A). In LMs, granular materials with low wettability are not dispersed in the liquid, but are adsorbed at the surface. Moreover, their grain size is significantly smaller than that of droplets and their density on the droplet surface is sufficiently high to prevent liquid spills (Fig. 1A). In most reports, LMs are typically millimetric water droplets covered with nano- to micrometre-sized hydrophobic particles. However, some studies have described the development of LMs using oil or solvents encapsulated with fluorinated (oleophobic) particles.[3] Regardless of the nature of the inner liquid, the LM particles stabilise an air layer, known as the Cassie–Baxter interface, around the droplet, which prevents liquid adhesion and allows the LM to easily roll off from a solid substrate or float on a liquid pool (Fig. 1B).

Moreover, LMs exhibit shape reconfigurability and can be split or merged repeatedly (Fig. 1C). This shape reconfigurability is unique to LMs, and it is impossible for droplets encapsulated with a bulk film. This indicates that LMs behave as soft solids in the static state. However, they can be split or merged like a fluid by applying a sufficiently strong mechanical force. Thus, LMs resemble a shear-thinning or thixotropic non-Newtonian fluid. Owing to these features and the wide range of possible liquid/particle combinations, LMs have received considerable attention and have been investigated in relation to various interesting domains; accordingly, various LM applications for replacing the inner liquid with fluidic media have been proposed. The wettability of the liquid medium to particles, which is mainly governed by the surface tension, determines the formation of LMs. Examples of liquid media include acidic/alkaline water, cell culture medium, glycerol,

fatty acids, organic solvents such as alkanes and alcohols, adhesives, blood, liquid food, ionic liquids, and liquid metal.[4–6] The liquid surface tension must be large enough to exhibit low wettability to particles. Moreover, liquid viscosity should be sufficiently low for the ease of droplet formation.[7,8] By using various functional liquids inside, LMs have been implemented in the fields of chemical reactors, sensor platforms, soft robotics, healing agents, and biosystems realised on a droplet scale; accordingly, they minimise liquid waste.[9,10] The outer particles of LMs are repeatedly used owing to the low wettability between the particles and the inner liquid (recyclable).[11–13] The easy recyclability of outer particles and lossless inner liquid transportation make LMs a promising technology for achieving a circular economy. Hence, the physical properties of LMs, such as multilevel robustness based on the application environment, have been intensively studied.[14,15]

Moreover, LMs with functional capabilities have been explored; for example, stimuli-responsive marbles that enable applications such as remote-controlled locomotion or regulated release of the inner liquid. The responsive behaviour of LMs has been observed using particles that respond to different triggers, such as light, electrical signals, magnetic fields, ultrasound, temperature, pressure, or chemical species.[16,17] Notably, LMs have attracted scientists working on hydrophobic coatings. Indeed, conceptually, both LMs and superhydrophobic surfaces can be regarded as hydrophobic structures forming an air layer at an interface, whether a liquid or solid, for LMs and superhydrophobic surfaces, respectively.[18,19] The similarities and differences between droplets on the superhydrophobic surface and LMs are discussed in section 2.

Researchers in the field of colloidal science treat LMs as liquid-in-air emulsions stabilised by particles.[20] Beyond the development of LMs, their potential applications have stimulated multidisciplinary research in various fields, including

Pritam Kumar Roy

Pritam Kumar Roy earned his MSc and PhD in Physics from IIT Kanpur. During his PhD, he worked on wetting tunability on soft solid and lubricant-infused surfaces under the supervision of Prof. Krishnacharya Khare. In 2019, he joined Prof. Edward Bormashenko's group at Ariel University, Israel, where he explored magnetic field-induced droplet movement and liquid marbles. He was awarded the Study in Israel Fellowship (PBC Fellowship) in 2020 and a JSPS Postdoctoral Fellowship in 2023. Currently, at The University of Tokyo with Prof. Timothée Mouterde, he studies non-contact droplet bouncing on lubricant-infused surfaces.

Koichiro Uto

Koichiro Uto is an independent scientist at the Research Center for Macromolecules and Biomaterials at the National Institute for Materials Science (NIMS) where he joined in 2018. He received his Ph.D. degree from Kagoshima University under the guidance of Prof. Takao Aoyagi. His postdoc research was performed with Prof. Cole A. DeForest and Prof. Deok-Ho Kim at the University of Washington. In 2016, he moved to NIMS as an International Center for Young Scientists (ICYS) researcher and became an AMED-PRIME researcher. His research interests include materiobiology, shape memory polymers and 4D printing technology for biomedical applications.

Fig. 1 Fundamentals and overview of recent research fields in liquid marbles. (A) Criteria to design LMs and scanning electron microscopy (SEM) image of a LM. The particles used are hydrophobic fumed silica AEROSIL® RY 300 (Evonik, Germany). (B) Non-sticking property of 10 μL of LMs resting on the solid surface and floating in a water pool. (C) Shape reconfigurability of LMs. Splitting LMs into two and coalescing two LMs into one is possible. (D) Research field of publications regarding LMs from June 2020 to 2023, obtained with the keyword "liquid marble" from Scopus Copyright © Elsevier BV.

materials science, physical chemistry, colloidal science, biology, and nanotechnology. Several review articles have reported the formation of functional LMs along with their physical properties and biochemical applications.[14,21,22]

Significant research progress has been made in the past three years in the field of LMs. According to our survey on reports on LMs, as shown in Fig. 1D, around 200 papers were published between June 2020 and June 2023, which included several stimulating discoveries, new LM concepts, fabrication processes, LM-templated design, and lab-in-a-marble applications such as microreactors, sensors, and biosystems.

This review covers the recent developments in LMs, mainly works reported after 2020, and highlights cutting-edge scientific findings on the physical properties of LMs, concepts, formation methods, LM-templated material design, and critical applications of lab-in-a-marble. We believe this work will help readers gain a comprehensive understanding of the current and potential development of LMs and related applications. To make this review understandable to general readers, we first review the fundamental properties of LMs in the following section.

2. Physical properties

2.1 Droplets and LMs

Nonwetting states can be achieved by forming an air layer between the solid and the liquid, for example, by patterning

either the substrate or the liquid (Fig. 2A). When a nonwetting state is achieved through substrate patterning, it is referred to as the superhydrophobic state.[23,24] A water droplet deposited on such surfaces forms a small sphere resembling a pearl. Meanwhile, LMs refer to the realisation of a nonwetting state by patterning a liquid with particles.[2] The similarities between these two nonwetting states allow us to understand some physical properties of LMs as an extension of drops on superhydrophobic surfaces (pearls).[25] In this section, we describe the physical properties common to LMs and droplets on superhydrophobic surfaces before discussing the physical properties specific to LMs.

When Aussillous and Quéré first demonstrated the concept of LMs, they formed a LM by rolling a liquid droplet onto a hydrophobic particle bed. When particles are adsorbed on a liquid interface, the total system energy decreases owing to the minimisation of the surface energy, resulting in the formation of LMs.[26] More precisely, with R_p denoting the particle radius and θ the contact angle of the liquid on a particle, for each particle adsorbed on the interface, the system energy decreases by:

$$\Delta G = \pi \gamma R_p{}^2 (1 - |\cos \theta|) \tag{1}$$

where γ denotes the liquid–air surface tension. This simple calculation shows that both hydrophobic ($\theta > 90°$) and hydrophilic ($\theta < 90°$) particles can be utilised to form LMs;[9,27] additionally, a stronger decrease in surface energy is observed

Fig. 2 Fundamental and physical properties. (A) Schematic depicting a pearl (droplets on superhydrophobic surfaces) and LM; in both cases, an air layer is formed between the liquid and substrate. (B) Sketch of air layer formed by particles adsorbed on the LM surface. The air layer thickness, δ, depends on the particle radius R_p and liquid/solid contact angle θ. (C) Images of LMs and pearls made with water and lycopodium with volume 20 and 400 μL, respectively. (D), (E) Various LM shapes achievable with different particle sizes depending on the ratio between LM radius R and particle size S.[49,94] (F) Different scenarios illustrating how LMs break upon impact.[15] (G), (H), (I) and (J) Effects of adhesion and friction on the motion of LMs and pearls.[25,26] (K) and (L) Shape evolution of water droplets and LMs during phase change of the inner liquid.[66,67,71] (M) Depiction of salt crystallisation at the interface[77] and (N) self-propulsion of Janus marble in water bath during the evaporation of inner liquid from LMs.[81] Copyrights: (D) Reproduced from ref. 49 under CC BY 4.0 Wiley-VCH GmbH 2020; (E) reproduced from ref. 94 with permission from Wiley-VCH GmbH, Copyright 2019; (F) reproduced from ref. 15 with permission from Wiley-VCH GmbH, Copyright 2021; (H) and (I) reproduced from ref. 25 with permission from the American Institute of Physics, Copyright 2023; (J) reproduced from ref. 26 with permission from the Royal Society, Copyright 2006; (K) reproduced from ref. 66 with permission from the Royal Society of Chemistry, Copyright 2021; (L) reproduced from ref. 67 and 71 with permission from the Elsevier Ltd., Copyright 2018 and from the Elsevier, 2021; (M) reproduced from ref. 77 with permission from the American Chemical Society, Copyright 2021; (N) reproduced from ref. 81 with permission from the American Chemical Society, Copyright 2015.

for particle wetting properties between hydrophobic and hydrophilic surfaces. Here, θ can be estimated by microscopic observation of the gel-trapped or polymerized liquid–air interface[28,29] using SEM, environmental-SEM, or a digital

microscope. Force measurement techniques, such as colloidal probe atomic force microscopy, can also be used to measure θ.[30] Consequently, Zang et al. reported that LMs covered with particles with θ close to 90° exhibit the highest mechanical

robustness.[31] The particle size and wettability not only determine the adsorption energy but also control the distance from the liquid to the substrate, as depicted in Fig. 2B. The liquid/substrate distance, δ, can be typically represented as $\delta = R_p(1 - \cos\theta)$. Hence, if a liquid fully wets the particles (hydrophilic), i.e., $\cos\theta = 1$, the liquid comes in contact with the substrate and the LM becomes unstable. However, in a complete nonwetting situation, $\cos\theta = -1$ and the liquid/substrate distance is maximal, but the particles are not adsorbed on the surface, leading to insufficient mechanical stability. This phenomenon is analogous to the superhydrophobic state, in that the substrate structures govern the thickness of the air layer below the liquid. However, particle adhesion to the liquid should be considered in the case of LMs.

Fig. 2C depicts 20 and 400 µL of water placed on a superhydrophobic surface and as a LM made with lycopodium, respectively. The images reveal that for both nonwetting situations, the pearl and marble shapes are nearly identical. This enables us to derive the LM shape depending on its radius, R, by considering the case of a liquid in a pure nonwetting situation ($\theta = 180°$). In the case where the particle mass is negligible, the geometry of the LM for drops is determined by the capillary length $\kappa^{-1} = (\gamma/\rho g)^{1/2}$, where γ is the LM surface tension, ρ is the liquid density, and g is the acceleration of gravity.

LMs smaller than the capillary length ($R < \kappa^{-1}$) are observed to be spherical owing to surface energy minimisation. The radius of the contact zone with the substrate, R_c, can be easily derived. The liquid weight, $\rho g R^3$, is balanced by the Laplace pressure, γ/R, inside the spherical LM applied on the contact area, i.e., R_c^2: $\rho g R^3 \sim R_c^2 \gamma/R$. Hence, the contact radius of the LM is smaller than the capillary length:[2]

$$R_c \sim R^2 \kappa \tag{2}$$

LMs larger than the capillary length ($R > \kappa^{-1}$) are flattened by gravity, forming puddles of height $2\kappa^{-1}$. Owing to volume conservation, the contact radius can be obtained as $R^3 \sim R_c^2 \kappa^{-1}$; hence, the contact radius of large LMs[2] is given by:

$$R_c \sim R^{3/2} \kappa^{1/2} \tag{3}$$

However, it should be noted that the height of the LM is smaller than that of the droplet. This difference can be partially attributed to changes in the surface tension of the interface caused by the replacement of the liquid/air interface with a liquid/particle/air interface. The interactions between the encapsulating particles adsorbed on the LM and core liquid modified the force equilibrium at the surface, leading to an "effective surface tension", denoted by γ_{eff}. This effective surface tension tends to slightly modify the contact radius and can be accounted for by calculating the capillary length using this effective surface tension γ_{eff}. The adjusted surface tension plays a pivotal role in determining the stability, mobility, and other characteristics of LMs. Researchers have proposed various techniques, such as the pendant drop method, the maximum height method, shape analysis, capillary rise, and vibration analysis, to measure the effective surface tension.[26,32–42]

2.2 Particle size and LM shape

In the previous section, we considered the particles to be sufficiently small in comparison with LMs to ignore the size effects; nevertheless, the particle size and geometry affect the LM shape and stability. It has been reported that the size of particles and number of layers required to form marbles are related. Generally, coarser particles (>50 µm) tend to form monolayer LMs, whereas finer particles form multilayer LMs.[43–45] The stability of LMs is affected by particle coating, size, surface density, and volumetric mass density.[46] Moreover, larger particles can produce somewhat stronger LMs, as shown by studies that attempted to test various particle sizes.[47] Asaumi et al. reported that as the particle size increases, it enables a larger gap between the inner liquid and the supporting substrate, along with stronger capillary forces between the particles at the LM surface, leading to improved mechanical stability. However, this increase in particle size also results in greater weight, causing larger deformations and, consequently, making breakage easier.[43] The LM stability also depends on the subjacent surface hydrophobicity and interactions with the environment. Larger particles can mitigate the collapse of LMs by increasing the air layer between the inner liquid and the external environment.[47] Moreover, superhydrophobic surfaces strongly enhance the robustness and self-healing capabilities of LMs. The balance between small and large particles can optimise the LM stability and evaporation rates by filling the gap and enabling a denser particle layer. Fig. 2D shows the relation between the droplet size R and the plate size S. Fujiwara et al. pointed out that the shape and dimensions of LMs can be finely manipulated by adjusting the size ratio between the water droplet and the PET plate, along with controlling the number of plates adsorbed on the droplet.[48] Fig. 2E demonstrates that owing to the jamming of PET plates, LMs of various shapes can be prepared.[49]

2.3 Mechanical stability

Owing to the protective layer of particles, LMs are more resilient to external stimuli than pearls (droplets on superhydrophobic surfaces). The stability of LMs indicates their ability to withstand external forces and maintain integrity over time. These aspects are directly influenced by the properties of the core liquid and surrounding particles. As illustrated in Fig. 2B, the wetting characteristics and size of particles play crucial roles in controlling the distance between the adhesive core liquid and its surroundings. This air layer is essential for marble stability during impact or when subjected to external forces. Tenjimbayashi et al. reported that LMs on superhydrophobic surfaces are more mechanically stable during impact than those on substrates with other wetting properties.[50] They also reported that LMs could exhibit a reversible wetting transition from the capillary to the partial Cassie state on a superhydrophobic surface. However, this reversibility is lost when the surface is hydrophilic. Fig. 2F shows the fracture dynamics of particle-monolayer-stabilised LMs upon impacting a solid surface using high-speed microscopic imaging. Two distinct

breakage scenarios are observed, which depend on the LM's Weber number (We = $\rho U^2 R/\gamma$, where U is the impact velocity).[15] The first scenario involves crack-induced breakage, which occurs at moderate We values (We = 15–20). In this case, the particle shell below the LM cracks and the liquid interface spreads directly onto the solid. This increases the outer particle shell packing fraction, leading to a jammed interface, which eventually fixed the drop into a jammed shape far from the spherical shape expected for a liquid droplet. Conversely, at higher Weber numbers (We > 20), a water-penetration-induced breakage scenario occurs owing to particle/solid friction, while the bottom interface of the LM remains covered with particles; however, the hydrodynamic pressure is sufficiently high to allow the liquid to reach the bottom substrate. Consequently, the final LM shape is a portion of a sphere. This scenario resembles the superhydrophobic failure scenario upon droplet impact, such as the Cassie–Wenzel transition.[51,52] However, in contrast to the fixed superhydrophobic structure, the particle structure of LMs is not fixed and flows along the penetrated liquid. As a result, the final state of broken LMs can be divided into a dry, pendular, funicular, capillary, or saturated state depending on the liquid saturation degree.[53]

2.4 Adhesion and friction of LMs

The most noticeable property of LMs is their high mobility, which is a hallmark of their nonwetting state. This enables easy fluid manipulation at the millimetre scale, where capillarity usually makes the droplets sticky. High mobility is a combination of low adhesion, which quantifies the force required to move LMs from rest, and low friction, which characterises the force necessary to move LMs at velocity V.

First, we discuss the adhesion mechanism of LMs. Although their shape resembles that of pearls on superhydrophobic surfaces, Jin *et al.* recently discovered that their adhesion is surprisingly different.[25] Drops larger than the capillary length placed on a superhydrophobic surface tilted at angle α start to move when the weight ($\rho g R^3 \sin \alpha$) is larger than the contact angle hysteresis adhesion ($\gamma R_c \, \Delta\cos\theta$). Substituting R_c with its value from eqn (3), the sliding angle, $\alpha^\star$, of large drops scales with $R^{-3/2}$ as follows:

$$\alpha^\star \sim \Delta\cos\theta \, (R\kappa)^{-3/2} \tag{4}$$

In contrast to the drops, the sliding angle of LMs does not depend on their volume (hence, mass) (Fig. 2H). The adhesion of LMs is fundamentally different owing to the solid/solid adhesion between the particles and the substrate. The maximum dry friction tangential to the surface is $\mu \, \rho g R^3 \cos\alpha$, where μ is the particle/substrate static friction coefficient and $\rho g R^3 \cos\alpha$ is the normal force distributed on the grains below the marble. LMs start to move when the weight ($\rho g R^3 \sin\alpha$) overcomes Coulomb adhesion; hence, its sliding angle is given as follows:[25]

$$\tan\alpha^\star \approx \mu \tag{5}$$

When moving on an incline at velocity V, the friction of LMs depends on the particle/substrate interaction, inner liquid viscosity, and surrounding gas. In the practical case of water, large LMs move at velocities in the order of 1 m s^{-1}. In this regime, the surrounding air is the main source of dissipation, making the LM velocity independent of the inner liquid viscosity (Fig. 2I). Friction arises from dissipation in the boundary layer surrounding the LMs (skin-drag friction), leading to a descending velocity:

$$V \sim (\gamma\rho g\kappa^{-1}/\eta_a\rho_a)^{1/3} \sin^{2/3}\alpha \tag{6}$$

where η_a and ρ_a denote the air viscosity and density, respectively. This regime was also observed in droplets running down a superhydrophobic incline;[54] however, the particle shell modifies the boundary conditions around the LMs (liquid/gas for pearls and solid/gas for LMs), leading to a slight decrease in the velocity of LMs.[25]

The difference between pearls and LMs disappears when the inner liquid viscosity becomes sufficiently large to dominate other friction forces. Thus, the two friction regimes can be distinguished based on the LM size. Large marbles flattened by gravity ($R > \kappa^{-1}$) roll, while the viscous friction due to the velocity gradient across the puddle of thickness κ^{-1} scales as $R_c^2\eta V/\kappa^{-1}$, which when balanced by weight $\rho g R^3 \sin\alpha$ leads to descending velocity inversely proportional to the liquid viscosity (Fig. 2I) and independent of the volume:[2,25,55]

$$V \sim \gamma/\eta \sin\alpha \tag{7}$$

The friction of small LMs ($R < \kappa^{-1}$) is still dominated by the viscous dissipation of the inner liquid. However, owing to their spherical shape, their rolling motion is similar to solid body rotation, which restricts viscous dissipation to volume R_c^3 next to the deformed contact, leading to descending velocity:[2,56]

$$V \sim (1/\kappa R) \, \gamma/\eta \sin\alpha \tag{8}$$

Counterintuitively, the LM velocity increases when the LM radius decreases; the LM weight driving the motion decreases, and the LM is observed to move faster owing to the fast shrinking volume over which viscous dissipation occurs (Fig. 2J).

A unique case arises when nanometre-sized LM particles form a monolayer. In this case, intermolecular forces can lead to direct liquid–substrate contact, resulting in a distinctive movement behaviour.[57]

2.5 Shape evolution *via* phase changes in the inner liquid

Evaporation plays a critical role in the practical use of LMs because it may cause shape deterioration and collapse.[58,59] This is particularly observed in the field of biomedicine, where heat cycles are used to cultivate cells inside LMs. Several research groups have investigated LM evaporation and analysed the effects of different coating particles and arrangements.[60–62] Despite the importance of the enclosed liquid volatility,[63] studies have demonstrated that the choice of coating particles can significantly modify the evaporation rate.

For example, a LM coated with graphite exhibits slower evaporation than bare water droplets, thus doubling its lifespan.[60] By contrast, the use of hydrophobic polytetrafluoroethylene microparticles (µPTFE) on LM's water–air interface only slightly prolongs its lifetime.[62] The roles of particle size and aggregation in LM evaporation have also been explored. Bhosale *et al.* noted that water diffusion through the LM shell is not solely tied to the particle size, suggesting the importance of aggregation.[64] Similarly, Laborie *et al.* proposed that the evaporation rate is not exclusively determined by the particle size and speculated that multilayer coatings might involve nanoparticle aggregates.[65] Understanding the intricate relationship between LM evaporation and the coating structure remains a focal point. A recent study by Mishra *et al.* combined theory and experiments to highlight that the interplay between liquid/particle and particle/particle interactions can result in three distinct residue shapes of marbles during evaporation (Fig. 2K).[66]

Phase changes in the core liquid, such as freezing, are also affected by particles that form the LM. A water droplet placed on an extremely cold surface freezes into a sharp-tipped ice drop, as shown in Fig. 2L.[67–70] This suggests that LMs filled with water adopt a similar shape after freezing. However, frozen LMs form three distinct shapes: conical, spherical, and flattened.[71] Interestingly, these shapes are not determined by the thermal or elastic properties of LMs. This diversity can be attributed to the different pinnings of contact lines during cooling. The pinning strength depends on the adhesion of coated particles to the cooled solid substrate. When the contact line is strongly pinned, it promotes the formation of freezing-tip singularity. Conversely, weak pinning leads to the creation of flattened shapes.

2.6 Evaporation-induced effects

The particle shell of LMs is not homogeneous, allowing mass transfer between the core liquid and the external environment. This mass transfer can occur through processes such as evaporation, osmosis, or manual injection of the liquid into the marble.[66,72–74] Evaporation of the core liquid leads to shape changes and other intriguing phenomena, including self-propulsion, interfacial crystallisation, coffee stain effects, and dewetting.[75–80] Fig. 2M illustrates the controlled asymmetric crystallisation of NaCl salt during the evaporation of the core liquid of a Janus marble coated with PTFE and carbon black and filled with a saturated saline solution.[77] It has also been reported that LMs filled with alcohol solution can self-propel when placed in a liquid bath, as shown in Fig. 2N. Self-propulsion arises from the Marangoni solute-capillary flow, which occurs owing to the condensation of alcohol that has evaporated from the LM onto the water surface.[81]

3. LM formation process

3.1 Material requirements

Here, we highlight the LM formation process. The formation of LMs is not technically difficult because it only requires droplets to be covered with low-wettability particles. The preparation of low-wettability particles is not challenging owing to the well-developed hydrophobic materials science (since the 1900s).[82,83] In early research, LMs were made using naturally or commercially available hydrophobic particles, such as lycopodium, PTFE, PVDF powder, carbon black soot, tonner particles, nanocarbons, fumed or colloidal silica nanoparticles, PS, PET, PDMS, wax particles, or long alkyl chain fatty acids. Some researchers focused on the formation of original hydrophobic particles (*e.g.*, hydrophobically modified metals, metal oxides, MOFs, non-commercial polymers, and/or composite particles) to form functional LMs with properties that could not be obtained using commercially available particles.[84]

3.2 Classical methods

Fig. 3A shows the two classical methods used to form LMs: (i) covering droplets with particles by letting the liquid roll off a tilted particle bed[2] and (ii) electrostatic adsorption of charged particles by applying a voltage difference between the particle bed and droplet.[85] In the former roll-off method, the droplet surface in contact with the particle bed adsorbs the particles, and the droplet becomes a LM. Several variations of this fabrication technique have been proposed, including the gentle placement of droplets, impacting, or spraying.[61,86] In the electrostatic method, particles on an electrically biased substrate jump to a liquid droplet when the liquid/particle distance is sufficiently small for the electric field to move the particles. Recently, several new LM fabrication methods have been proposed, including the massification and miniaturisation of production for practical applications, complex particle patterning, and the use of different physical phenomena. The new fabrication methods, summarised in Fig. 3B–E, may contribute to the diversification of the concept of LMs and improved productivity.

3.3 Small LM formation

The concept of massive formation of tiny LMs using a superhydrophobic mesh is shown in Fig. 3B.[87] Small droplets were formed by the segmentation of a water pool passing through the pores of a superhydrophobic mesh. The droplets were then spontaneously coated with hydrophobic particles that were previously placed on the mesh to form LMs. Consequently, thousands of submillimetre LMs were formed simultaneously, and their sizes could be controlled through the mesh size.

Moreover, Lekshmi *et al.* reported the formation of submillimetre LMs by splitting LMs based on mechanical impact (Fig. 3C).[88] When a droplet impacts the particle bed at a sufficiently high velocity (high Weber number), the droplet bounces to split/form tiny satellite droplets; after two consecutive splits, the LM diameter reaches the submillimetre scale.

3.4 Janus LM formation

While most LMs are covered with one type of particle, the shells of Janus LMs are composed of regions made of different types of particles. Janus LMs are generally formed by the coalescence of two LMs with different particle types. However,

Classical methods

A Roll-off — Droplet — Electrostatic — Tilted particle bed

Massive LM formation by droplet fragmentation

B Powdered superhydrophobic mesh — Tap

Tiny LM formation from satellite droplet

C LM (microliter) — SLM (sub-microliter) — Satellite PLD

Janus LM production

D Particle laden drop (PLD) — Sequentially produced JLMs — BTP bed — Rotating platform

LM formation by thermal flow

E water drop — levitating clusters — copper block electric heater — $T = 573$ K

Fig. 3 Recent progress in LM formation methods. (A) Classical LM formation method: roll-off (left) and electrostatic methods (right). (B) Massive formation of tiny LMs by applying impulsive pressure to powdered superhydrophobic mesh on water pool.[87] (C) Formation of tiny LMs by covering the impacting satellite droplets with particles.[88] (D) Continuous formation of Janus LMs by impacting a particle-laden droplet onto other types of particle beds.[89] (E) Covering droplets with thermally levitating nanoparticles.[90] Copyrights: (B) Reproduced from ref. 87 with permission from the American Institute of Physics, Copyright 2023; (C) reproduced from ref. 88 with permission from the American Chemical Society, Copyright 2022; (D) reproduced from ref. 89 with permission from the American Chemical Society, Copyright 2020; (E) reproduced from ref. 90 with permission from Elsevier, Copyright 2022.

it is difficult to mass-produce LMs using this formation process. Janus LMs can be formed by LM impacts on surfaces covered with different types of particles (Fig. 3D).[89] When LM impacts the particle bed, it deforms and a part of the inner liquid surface is exposed.[50] The LM becomes heterogeneous when a second type of particle is attached to the exposed liquid surface. The study in Fig. 3D controlled the impacting behaviour of the fluorine polymer-covered LM on a black toner particle bed to form Janus LMs. The studies introduced in Fig. 3B–D were based on the physical adsorption of particles based on the direct contact of droplets, and several developments in the formation process are expected to form more complex patterns.

### 3.5 Particle-heating-induced LM formation

While the indirect particle adsorption method was first limited to the previously described electrostatic method (Fig. 3A), the work presented in Fig. 3E proposed another indirect LM formation method[90] based on thermal flow-induced particle levitation. When a bed of low-density nanoparticles is heated to sufficiently high temperatures (here, 300 °C), the nanoparticles levitate driven by thermal flow and get adsorbed on the droplet surface to form LMs. Overall, simple and convenient LM formation methods have been recently developed.

4. Conceptual variation in LMs

Since the first report on synthetic LMs in 2001,[2] various studies have attempted to analyse functional LMs based on responsive particles.[16] These studies mostly fit within the category of classical LMs in terms of size, with millimetric and outer granules being powders. Concurrently, attempts to change the shape of granules have been reported. For example, in 2014, Miao *et al.* reported that LMs can be stabilised by silver nanofibers.[91] In 2019, Geyer *et al.* reported a polyhedral LM, wherein a droplet was covered with millimetric polyhedral polymer plates to form a soccer-ball-like morphology.[49] Owing to the diversity of colloid shapes reported thus far,[92,93] the LM with non-spherical granules presented a new avenue for designing LMs with unfamiliar shapes, and various subsequent works have been reported.[76,94] However, conceptual variation is not limited to the particle shape.

4.1 Micro-LMs

Interestingly, since 2020, several studies have proposed conceptual variations in LMs with original LM compositions or morphologies. Such new concepts may inspire further research on LMs. Here, we summarise the conceptual variations in LMs (Fig. 4). While the LM size is usually on the millimetre scale, a recent work, displayed in Fig. 4A, reported the massive production of LMs with sizes in the range of single to hundreds of micrometres. This work allowed the isolation of a single micrometre-sized LM, enabling micro-LM handling, as shown in Fig. 4A. It is noteworthy that a large number of such micro-
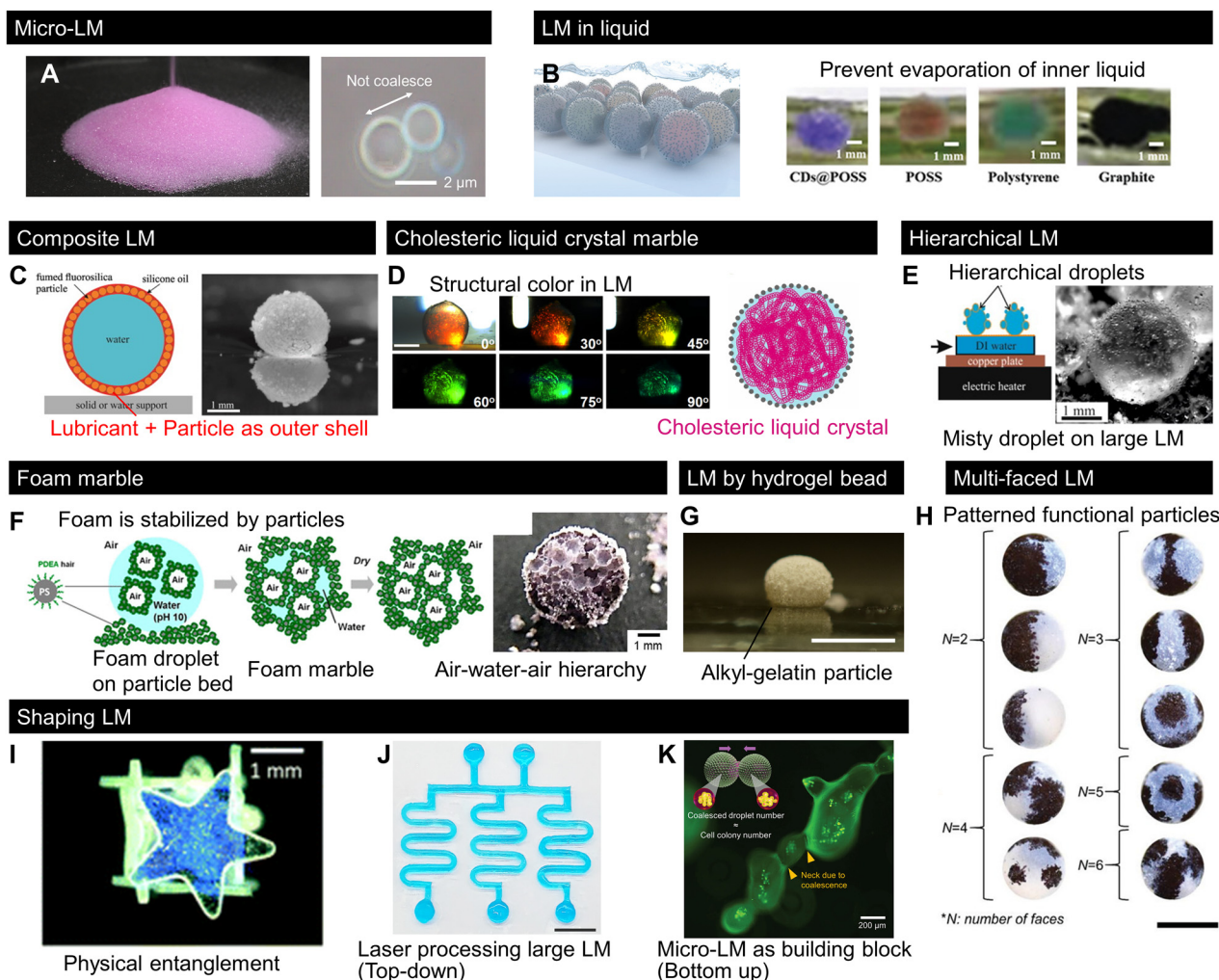
Fig. 4 Recent progress in LMs with uncommon shapes, structures, and compositions. (A) Mass LMs downsized from a single micrometre to hundreds of micrometres behave like dry powder.[13] (B) LMs sink into an immiscible liquid pool to prevent inner liquid evaporation.[97] (C) LM covered with lubricated particles, namely composite LMs.[99] (D) LM with a cholesteric liquid crystal core exhibit a structural colour change.[103] (E) LM covered with tiny droplets, namely hierarchical LM.[104] (F) LM made of foam resulted in air–water–air type LM.[105] (G) LM composed of hydrogel particles.[106] (H) Particles multipatterned on droplets using a patchwork-like process.[110] (I) LM made of a shaped solid. The physical entanglement of shaped solids deforms the droplets.[113] (J) Laser-processed nonspherical millimetric LM.[114] Scale bar: 1 cm. (K) Non-spherical micro-LMs formed by LM coalescence.[13] Scale bar: 200 μm. Copyrights: (A) and (K) Reproduced from ref. 13 with permission from Wiley-VCH GmbH, Copyright 2023; (B) reproduced from ref. 97 with permission from Wiley-VCH GmbH, Copyright 2020; (C) reproduced from ref. 99 with permission from Elsevier, Copyright 2020; (D) reproduced from ref. 103 with permission from Wiley-VCH GmbH, Copyright 2020; (E) reproduced from ref. 104 with permission from Elsevier, Copyright 2022; (F) reproduced from ref. 105 with permission from the American Chemical Society, Copyright 2022; (G) reproduced from ref. 106 under CC BY 4.0, MDPI 2022. (H) Reproduced from ref. 110 with permission from Wiley-VCH GmbH, Copyright 2021; (I) reproduced from ref. 113 under CC BY 3.0, 2021 the Royal Society of Chemistry; (J) reproduced from ref. 114 under CC BY 4.0, 2023 Springer Nature Limited.

LMs behave like granular materials.[13] It has been known that microdroplets are held in a hydrophobic particle network, the so-called dry liquid.[95,96] The micro-LMs are isolated to a single droplet from the hydrophobic network in a stable state; additionally, the size of the micro-LMs is uniform after the sintering process.

4.2 Wet LMs

Although LMs are generally handled in air, the work presented in Fig. 4B reported the use of LMs in liquids.[97] LMs in liquids are analogous to Pickering emulsions that are stabilised by

particles;[98] however, marbles in the millimetric scale can be isolated and handled as single droplets. The authors showed that LMs in liquids can be used to prevent the evaporation of the LM content, which is useful for applications requiring long-term stability.

Fig. 4C shows a new concept for composite LMs in which a water droplet is covered with both an immiscible lubricant and particles.[99] Similar to the case of lubricant-infused surfaces, where a lubricant layer was stabilised by capillary interactions with the surface structures,[100–102] in composite LMs, a stable lubricant/particle layer was formed at the interface of

these composite LMs. Accordingly, composite LMs exhibited higher interfacial stability, allowing them to bounce from a vibrated liquid bath, and the lubricant layer decreased the effective surface tension while increasing the surface viscous dissipation.

4.3 Liquid crystal marbles

Optical soft materials also benefit from the new concepts of LMs. The work presented in Fig. 4D introduced a LM with aqueous hydroxypropyl cellulose solution as the inner liquid.[103] While this may seem to be a simple variation of the inner liquid of a LM, hydroxypropyl cellulose self-assembles as a cholesteric liquid crystal in the aqueous phase. By regulating the cholesteric pitch in the LM, LMs with various structural colours were successfully fabricated. This unfamiliar photonic response of LMs contributes to variations in optically soft materials.

4.4 Hierarchical LMs

The approach presented in Fig. 4E comprises a hierarchical LM, which is covered with smaller droplets or LMs.[104] They can be formed by forming a particle bed at the surface of a hot water bath. Hot water vapour recondenses on the hydrophobic powder, forming LMs that then stick to neighbouring LMs, giving rise to hierarchical LMs.

While hierarchical LMs are made of different liquid parts, a recent work (Fig. 4F) demonstrated "foam" marbles comprising a hierarchical structure of LMs with alternating liquid and air contents, formed by covering the foam with hydrophobic particles.[105] This foam marble had a double emulsion-like feature, i.e., particle-stabilised air bubble-in-liquid and liquid droplet-in-air (air/liquid/air type). After drying, the foam marbles formed porous spheres with pore sizes of tens of micrometres.

4.5 LMs by soft particles

Fig. 4G shows a LM composed of soft hydrophobic gelatine particles.[106] The material properties of LMs have been studied by changing their particle size, shape, and/or surface chemistry.[20,43,107] Because recent studies have revealed that solid softness varies the interfacial energy balances, called soft wetting,[108,109] the LM based on a soft solid provides new opportunities to explore the effects of softness on LM properties.

4.6 Multi-faced LMs

As mentioned in the fabrication section, patterning LMs with different types of particles introduces new possibilities for various applications. The work presented in Fig. 4H demonstrated the possibility of fabricating complex patchworks with different functional particles on the surface of the liquid. The fabrication procedure allows flexible engineering for a wide range of patchworks.[110] In contrast to fluid instability, such as Rayleigh–Benard which allows the formation of complex fluid patterns, it is difficult to pattern granules because of their scale.[111] Thus, conventional patterns on the surface of LMs remain rather simple (e.g., Janus LMs; Fig. 3C).[112] Multi-faced LMs also provide insights for precise patterning with functional particles on the droplet, namely "multi-faced LMs", which provides the synergetic functionality to LMs that cannot be achieved by simply mixing functional particles.

4.7 Non-spherical LMs

We have shown in Fig. 2D that various granule shapes along with different droplet/granular size ratios. Small nonwetting droplets are spherical owing to surface energy minimization; however, the presence of particles at the surface of LMs allows the formation of non-spherical LMs. Fig. 4I–K illustrate different approaches used to shape LMs.[13,113,114] The first method, presented in Fig. 4I, reported a box-shaped droplet covered with a millimetric star-shaped plate.[113] Here, the plates were physically entangled with each other, making the droplets nonspherical. This concept is analogous to capillary origami[115] or capillary containers.[116] In this case, LM shape reconfigurability was strongly hindered; however, this LM exhibited high mechanical robustness. Li et al. proposed another method to deform droplets based on the interfacial jamming of nanoparticles on the droplets.[117] Fig. 4J shows the laser-based shaping process of a large LM with a specific geometry.[114] While the laser technique is a top-down approach for LM shaping, Fig. 4K shows a bottom-up shaping approach through the formation of non-spherical LMs by merging micro-LMs as building blocks.[13] This method enables the fabrication of complex marbles with micrometric dimensions, such as microfiber-shaped LMs formed by the coalescence of a micro-LM line. These new concepts are expected to give rise to unexpected LM properties, systems, and applications. Finally, among the new concepts, there is an increasing interest in the mechanical properties of LMs and LM assemblies to produce more complex structures.
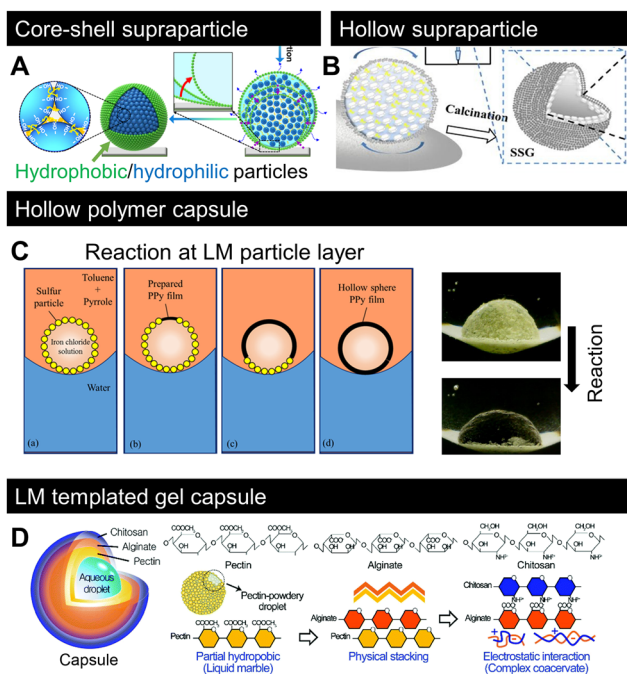
5. LM-templated material design

5.1 Supraparticle synthesis

Fig. 5 shows the recent advances in material design based on LMs as "templates". The first approach displayed in Fig. 5A and B involves particle adsorption at the liquid interface as well as controlled evaporation to arrange and position particles and polymers to form complex supraparticles.[118,119] Both methods utilise the low adhesion of the LM contact line to the substrate (Fig. 2M). The method displayed in Fig. 5A involves covering an aqueous solution of hydrophilic polymers/particles with hydrophobic particles to form a LM. Then, the inner water evaporates, and owing to the receding contact line, the inner particles/polymers become concentrated and form a complex biphilic supraparticle known as (hydrophilic)core–(hydrophobic)shell. As shown in Fig. 5B, the inner liquid content was removed via calcination to form hollow (air-core) supraparticles. A similar study was reported for the droplets of a colloidal dispersion deposited on a superhydrophobic surface; evaporation and the absence of contact line pinning

Fig. 5 Recent progress on LM-templated materials. (A) Designing core–shell or (B) hollow supraparticles by removing the inner liquid from LM.[118,119] (C) Polymerisation of pyrrole on the LM surface by a chemical reaction between the inner liquid and surrounding media.[123] (D) LM-templated gel-capsule formation.[124] Copyrights: (A) Reproduced from ref. 118 under CC BY 4.0, 2023 Springer Nature Limited; (B) reproduced from ref. 119 with permission from Elsevier, Copyright 2022; (C) reproduced from ref. 123 with permission from Elsevier, Copyright 2021; (D) reproduced from ref. 124 with permission from the Royal Society of Chemistry, Copyright 2020.

allowed the formation of supraparticles.[120–122] However, this method does not enable the formation of core–shell type supraparticles that make LMs a valuable tool for forming such complex materials.

5.2 Interfacial polymerisation

Recent studies have demonstrated that LMs can serve as intermediate templates to form polymer capsules, as shown in Fig. 5C and D.[123,124] Fig. 5C shows that polymerisation occurred at the droplet surface. The monomer and initiator were supplied from the outer fluidic medium (in this case, toluene) and inner liquid (in this case, iron chloride). The idea of interfacial polymerisation based on LMs in air has been reported before.[125] However, the reaction occurs at the liquid–liquid interface, i.e., LMs in the liquid system (Fig. 4B) form a hollow polymeric sphere. As shown in Fig. 5D, LMs stabilised by pectin powder were physically stacked with alginate and then electrostatically covered with chitosan to form a polyion complex-like physical gel capsule. These studies demonstrated that LMs are flexible templates for designing complex materials. Although the products are limited to spherical LMs, recent advances in the shaping of non-spherical LMs (Fig. 4I–K) should enable the formation of templates for non-spherical materials.

6. Recent lab-in-a-marble applications

6.1 Lab-in-a-marble (LIAM)

We now discuss the recent cutting-edge LM applications. Several studies have attempted to conduct laboratory experiments such as material synthesis, analysis, and bio-culturing on a small scale. Owing to the advances in microfluidics through the concept of "lab-on-a-chip",[126] which is beneficial for waste reduction (both liquid and equipment) through miniaturisation, this domain has been strongly developed in recent years. While recent microfluidic devices have many gimmicks for complex material synthesis and analysis, they require the formation of specific fine microfluidic channels through dry processing and the use of high injection pressure to pump fluids.[127] Moreover, the wastage of processed channels may lead to an environmental burden. Recently, the research field studying microfluidics and fluid-structure interactions, namely micro elastofluidics, has greatly developed.[128] In elastofluidics, LMs are waste-free fluidic systems owing to their recyclable outer particles and non-spilt inner liquid. Thus, it can be potentially used in a new class of laboratory experiments at the droplet scale with applications similar to that of microfluidic devices, known as "lab-in-a-marble (LIAM)". Various applications based on LMs have been reported thus far, including reactions, analysis, sensing, and energy conversion.[129,130]

6.2 Design strategies

The typical LIAM strategies are summarised in Fig. 6A and B. As exemplified by microfluidics, droplet-scale lab analysis first requires displacing and bringing several chemical species or biomaterials in contact with each other, which is one of the features of LMs owing to their low friction and coalescence capability. Additionally, to further process the liquid content, the liquid must be divided into smaller volumes to enable different characterisations or parallelise the subsequent steps of the process. This is also possible in LMs owing to their reconfiguration capabilities, because of which they can be easily split into sub-LMs. In addition to the fluid manipulation capabilities of LMs, Fig. 6A describes LM-specific advantages for a droplet-scale laboratory. While LMs can be used as standard microchemical reactors by merging the content of two LMs, the outer hydrophobic particles, whose primary function is to stabilise the liquid, can also be used to modify the reactor capabilities of LMs. Some studies have demonstrated the use of specific particles to assist reactions owing to their catalytic or reactive properties.[91,131] Moreover, in contrast to microfluidics, where droplets are enclosed inside liquid and solid channels, the open geometry and porous particle interface enable the use of a wider range of stimuli with LMs. For example, gaseous chemicals, light, and heat sources can be employed to trigger and/or enhance reactions inside LMs.[64,132] This sensitivity to stimuli may be related to the density and thickness of LMs.

Fig. 6 Recent progress in LM for microreactors, sensors, and actuators. Typical strategies for using LMs as (A) reactors, or (B) sensors and actuators.[138,139] The inner liquid is mixed by LM using (C) rotation or (D) oscillation. (E) Cascade chemical reaction using LM with a preprogrammed lifetime on a liquid pool.[140] (F) Contactless detection of LM properties by electroanalysis using a comb electrode.[141] (G) LM-based actuator. The photoresponsive motion of LM was used to actuate the locomotion of soft objects.[142] Copyrights: (C) Reproduced from ref. 138 with permission from the Royal Society of Chemistry, Copyright 2022; (D) reproduced from ref. 139 with permission from the American Chemical Society, Copyright 2022; Є reproduced from ref. 140 with permission from Wiley-VCH GmbH, Copyright 2023; (F) reproduced from ref. 141 with permission from the Royal Society of Chemistry, Copyright 2019; (G) reproduced from ref. 142 with permission from Wiley-VCH GmbH, Copyright 2023.

LMs can also be used as sensors or actuators, as shown in Fig. 6B; in this strategy, a responsive species is used as either a particle or within an inner liquid. If a responsive LM is used to quantify, visualise, or detect stimuli, and then the LM works as a sensor. For example, LMs can be used as gas-sensing devices by loading them with a pH-sensitive solution, which changes colour in response to acidic or basic chemicals.[133,134] If the LM response to external stimuli is converted to kinetic energy, it functions as an actuator to transport liquids or pick up particles. Owing to their reconfigurable features, LM actuators can be used in soft robotic systems.[135]

6.3 Chemical reactors

Although various LM reviews have focused on LM applications,[10,136,137] we selected recent reports with unfamiliar insights into LM applications. While coalescence-based chemical reactions have been reported, the miniaturisation of LMs makes effective mixing methods between the reactants more important because the viscosity action dominates at a small scale. Fig. 6C and D show the LM mixing methods;[138,139] both studies successfully generated a flow designed to mix the

inner liquid *via* outer mechanical stimulation through rotation or oscillation.

6.4 Cascade reactions

While the LM content can be retrieved by a simple mechanical action, it is important to control its lifetime for liquid release. Recently, researchers successfully engineered particles to control the LM

lifetime in a liquid pool while remaining stable upon being deposited on a substrate.[140] The floating lifetime of LM is controlled by forming marbles with a particle layer made of nanoclays with different surface chemistries. By loading chemicals into floating LMs with different lifetimes, the encapsulated chemicals are released into the liquid pool with programmed timing, followed by cascade reactions, as shown in Fig. 6E.

6.5 Non-destructive LM sensing

The characterisation of LMs is important for applications, as shown in Fig. 6F, which focuses on sensing LM properties, including the particle size, liquid conductivity, volume, and

position.[141] The properties of LMs were detected using a comb electrode that measured the electrical response.

6.6 LM-based actuators

More original concepts based on LMs have recently been published, as shown in Fig. 6G, which displays the concept of robotic actuation driven by photo stimuli.[142] In this study, the photo-stimulated kinetic energy of LMs was used as the engine of a small robot to achieve photo-responsive locomotion. LMs operated as tiny kinetic energy converters. Although the conversion efficiency was not reported, this work demonstrated the potential of complex robotic systems.

6.7 Bioapplications

The physicochemical properties and structural uniqueness of LMs have attracted the interest of many scientists and demonstrated potential for bioapplications in addition to the aforementioned microfluidics, sensors, and actuators. Here, we present some examples of bioapplications based on LMs over the past few years on multiscale biological specimens ranging from nucleic acids and proteins to cells and mini-organs, and discuss the advantages of LMs over conventional methods (Fig. 7).

6.8 SERS detection

Noncovalent interactions play an important role in biological phenomena such as enzyme–substrate, DNA–drug, and host–pathogen interactions. Leong et al. fabricated plasmonic LMs consisting of Ag nanocubes functionalised with mercaptobenzoic acid (MBA) as a surface-enhanced Raman scattering (SERS) platform (Fig. 7A).[143] MBA immobilised on Ag nanocubes served as an interaction probe molecule; moreover, hydrogen bonding and ionic interactions with the carboxyl groups of MBA resulted in differences in the Raman spectra. Although conventional SERS studies are limited to detecting a single mode of interaction, the combination of plasmonic LMs with chemometrics and density functional theory enables the observation of multiple molecular interactions and successfully demonstrates that noncovalent intermolecular interactions with nucleotide bases can be detected in situ.

6.9 DNA amplification

Because typical LMs lack appropriate heating capabilities, their applications as reactors or in analytical fields are limited to room temperature or using heating equipment. Fe_3O_4 nanocube-coated LMs have been fabricated as heatable miniature reactors because their internal liquid phase can be uniformly heated when exposed to an alternating magnetic field (AMF).[144] Furthermore, because Fe_3O_4 nanocube-coated LMs allowed the desired temperature and heating/cooling program by the power and on/off switching of the AMF, they were applied as a miniature reactor for DNA amplification and achieved 25% better amplification compared to commercially available thermal cycling methods (Fig. 7B). Although photothermal LMs, wherein only the light-irradiated area is heated, have been reported, the use of the magnetothermal effect in

Fe_3O_4 nanocube-coated LMs results in more uniform heating and is expected to be used as a larger-scale reactor.

6.10 Protein analysis

LMs are promising not only as reactors for miniaturised biochemical reactions but also as platforms for protein analysis. Typical protein analyses require pretreatment owing to the complexity of samples, which is difficult to accomplish with simple LMs. However, Niu et al. addressed this problem by designing fluidic channels using deformable LMs, termed liquid plasticine (Fig. 7C).[145] Liquid plasticine takes advantage of the high structural and morphological flexibility of LMs; thus, it can be shaped into rod-like shapes that mimic channels. Using human serum samples, they successfully demonstrated that the combination of liquid plasticine-based channels and isoelectric focusing (IEF) can simultaneously accomplish the important pretreatment steps of protein separation and enrichment. After pretreatment with IEF, LMs containing proteins of interest were isolated by cutting the liquid plasticine, allowing further evaluation by colorimetry and mass spectrometry.

6.11 Cell cryopreservation

In addition to biomolecules such as nucleic acids and proteins, as described above, biological samples with larger sizes, such as cells, can be confined to the liquid phase of LMs. Liu et al. proposed a LM-based cell cryopreservation method (Fig. 7D).[146] They fabricated LMs composed of gelatine solution and hydrophobic PTFE powder, where the PTFE particle layer not only acted as a physical barrier to protect cells from the external environment, but also influenced ice formation and growth during the freeze–thaw process of the solution. Furthermore, LMs containing gelatine in the liquid phase do not require additives, such as dimethyl sulfoxide (DMSO), which is cytotoxic, and foetal bovine serum (FBS), which may cause pathogenic contamination, like conventional cell cryopreservation; gentle shaking immediately destroys LMs and allows recovery of cells, thereby achieving high cell viability after cryopreservation.

6.12 Single-cell picking

Recently, a cell-manipulation technique based on dry cells: cell-encapsulated micro-LMs, obtained by simply spraying a cell suspension onto a powder bed of hydrophobic fumed silica nanoparticles, was developed.[13] The number of cells to be encapsulated was determined by adjusting the size of LMs and the concentration of the cell suspension; accordingly, dry micrometre-sized cells were fabricated. These dry cells provided a venue for the isolation of single cells and observation of their cellular phenomena, such as migration and growth, in addition to utilising LMs as simple storage containers for cells (Fig. 7E). Cells sequestered under dry conditions showed a cell viability of approximately 90% for at least three days. The cellular phenomena can be analysed for longer periods owing to handling techniques such as changing the internal liquid (culture medium). Furthermore, by using the conditions of dry-cell formation and physical properties originating from
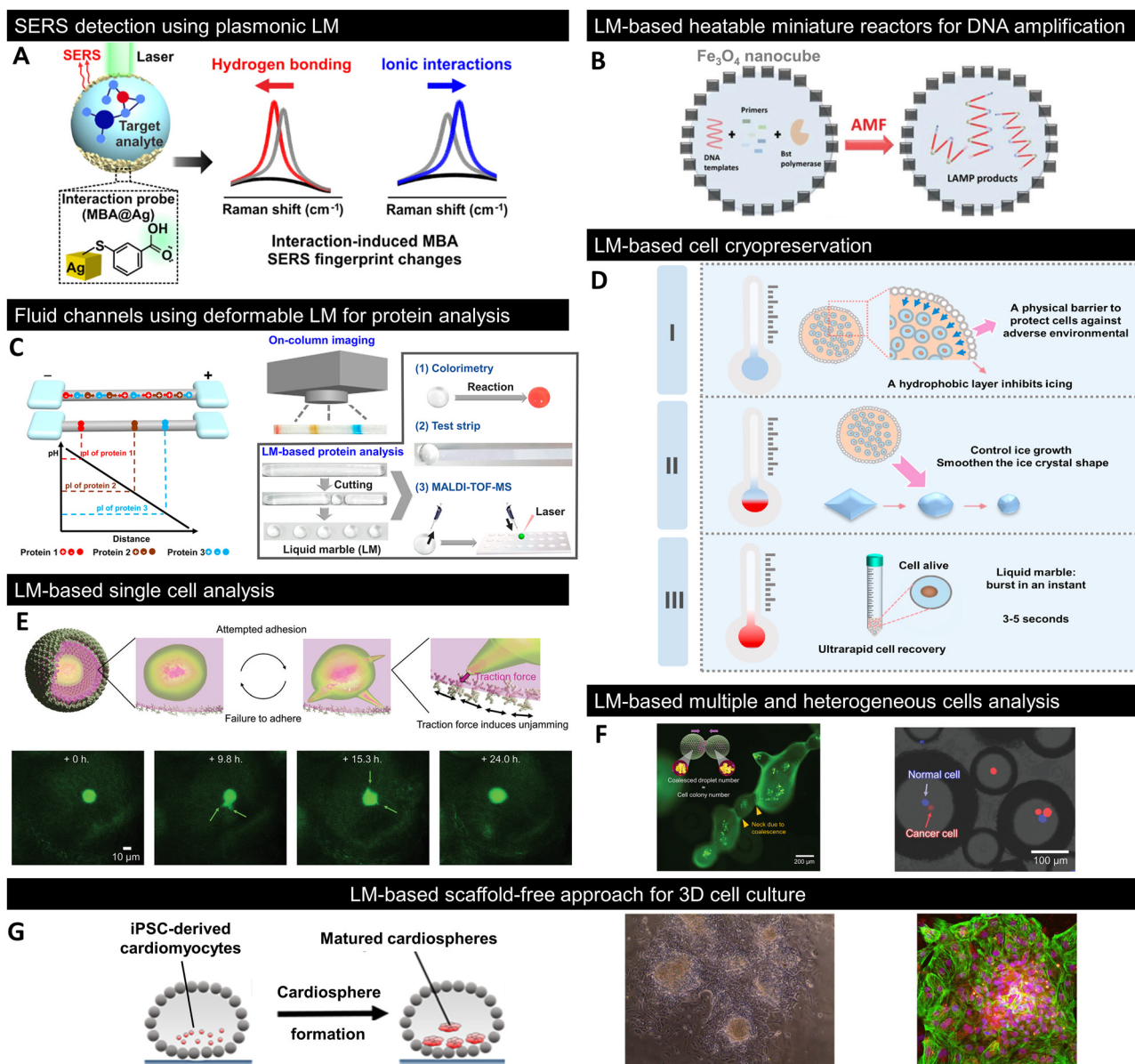
Fig. 7 Recent progress in LM for bioapplications. (A) *In situ* detection of noncovalent intermolecular interactions between MBA and the target analyte using plasmonic LMs.[143] (B) DNA amplification using Fe_3O_4 nanocube-coated LMs as an alternative magnetic field (AMF)-triggered heatable miniature reactors.[144] (C) Isoelectric focusing (IEF)-based protein analysis using fluid channels composed of deformable LM, termed liquid plasti-cine.[145] (D) Cryopreservation of cells using gelatine-based LMs and its mechanism.[146] DryCell technology is based on cell-suspension microscale LMs for the analysis and manipulation of (E) single and (F) multiple heterogeneous cells.[13] (G) LM-based scaffold-free bioreactor for the 3D culture of *in vitro* derived human cardiomyocytes.[150] Copyrights: (A) Reproduced from ref. 143 with permission from the American Chemical Society, Copyright 2020; Copyrights: (B) reproduced from ref. 144 with permission from Wiley-VCH GmbH, Copyright 2021; Copyrights: (C) reproduced from ref. 145 with permission from the American Chemical Society, Copyright 2020; Copyrights: (D) reproduced from ref. 146 with permission from Elsevier, Copyright 2022; Copyrights: (E) and (F) reproduced from ref. 13 with permission from Wiley-VCH GmbH, Copyright 2023; Copyrights: (G) reproduced from ref. 150 with permission from Elsevier, Copyright 2020.

LMs, various cellular environments can be created, including spatially arranged cell colonies induced by fusion and one-cell confinement of different cell types (Fig. 7F).

6.13 Three-dimensional cell culturing

Three-dimensional (3D) cell cultures more accurately mimic the *in vivo* environment and have several advantages over con-

ventional two-dimensional (2D) culture systems. Hence, studies have been conducted to utilise the liquid phase of LMs surrounded by a hydrophobic powder as an *in vitro* 3D culture field. Cells in the liquid phase of LMs tend to self-assemble to form spheroid- and organoid-like structures, which have been observed in C6 rat gliomas, human mammary fibroblasts, and human hepatocellular carcinoma cells.[147–149] Aalders *et al.*

were the first to apply LMs to the 3D culture of induced pluripotent stem cell (iPSC)-derived cardiomyocytes and succeeded in forming cardiomyocytes in less than 24 hours (Fig. 7G).[150] Cardiospheres formed inside LMs also expressed myocardial markers similar to those in conventional 2D culture systems. Further findings in LM-based 3D culture systems could provide a useful alternative to expensive and experienced scaffold-free 3D culture methods such as spinner flasks and hanging drops.

7. Conclusions

In this review, we comprehensively highlighted the recent progress in LMs. This literature review revealed that the latest research on LMs extends far beyond mere applications or novel particle/liquid combinations. Indeed, there is flourishing literature dedicated to new LM concepts, LM formation methods, understanding of LM physical properties, and LM-templated material design. The richness of the literature and emergence of several new LM concepts foreshadow the strong and rapid development in the LM field. In the fundamental physical analysis of LMs, the comparison of the mechanics and phase invasion behaviour between the droplet and LM offered us the opportunity to reconsider the physical properties of LMs. Moreover, while the initial LMs are conceptually similar to drops on superhydrophobic surfaces, the physical properties of new conceptual LMs are yet to be investigated. On the industrial side, the large-scale and reliable production of LMs remains a bottleneck. The recently developed LM formation method can largely solve this issue, making LMs more applicable in industries. Moreover, because the different fabrication processes of conventional LMs lead to a wide range of new LM concepts, we can expect the recently proposed fabrication process to bring its own variations, which will further broaden LM variations. The new LM concepts must expand the potential use of LMs. Non-spherical LMs can expand the use of LIAM to enable the design of complex systems, such as microfluidic devices, and hierarchical LMs or LM patchworks can be used to design new LM-templated materials. Focusing on LM applications, various advances in responsive LMs, evaluation methods, and energy conversion systems have been proposed, thus broadening the applicability of LMs. From the perspective of materials science, evolutive LMs can adapt their properties to resist their environment because recent research directions in materials science have shifted from simple responsive materials to designing adaptive or interactive materials similar to living objects, which are much more complex than responsive or intelligent materials and have gained considerable attention.[151] For example, a recently developed supermolecular chemistry-enabled self-training gel increases its tensile strength with breakage–healing cycles similar to that of muscle.[152] Thus far, responsive LMs have been studied mainly in the 2010s,[16] and in the future, LMs should be designed to have adaptative capacities. This may be achieved by liquid and particle engineering, which may help in obtaining LMs with fine-tuned responses to the environment. One may think that to design multiple liquids or particles, a cascade response or multilevel stability may be required. As discussed in multi-faced LMs, tuneable multi-responsivity can be achieved by combining multi-functional particles. The mixing ratio of several functional particles would likely be the key factor to achieve tuneable multi-functionality in LMs. Moreover, keywords used in LMs such as "reconfigurability" and "jamming transition" are included in designing recent adaptive materials systems.[153,154] For example, utilizing liquid reconfigurability, the concept of liquid-based adaptive structural materials (LASMs) has been recently proposed.[155] Thus, we believe that adaptive LMs can be designed by focusing on shape reconfigurability and interfacial jamming in LMs. The diversity of hydrophobic particles and liquid phases that constitute LMs has led to the design and development of various functional LMs for bioapplications that are challenging for conventional microfluidics systems. LMs can contain biological specimens of various sizes within a specific liquid space separated from the external environment, enabling the analysis of noncovalent intermolecular interactions, DNA amplification reactions, and rapid protein analysis. In addition to using LMs as miniaturized containers for biochemical reactions and storage containers for biological samples, they can be used to culture and maintain living organisms such as cells. In particular, single-cell analysis technologies that measure the genome, epigenome, transcriptome, proteome, and metabolome for each single cell have recently attracted significant attention to accurately understand single-cell level behaviour in the cellular society of embryogenesis, tissues, and organs. Because individual elemental technologies for bio-analysis, cell manipulation, and 3D culture for spheroid and mini-organ formation have already been established using LMs, the realisation of bioapplications using LIAM that integrate everything, from cell culture to analysis, would not be far off.

Author contributions

Mizuki Tenjimbayashi: project administration, supervision, conceptualization, investigation, visualization, writing – original draft, validation, and funding acquisition. Timothée Mouterde: supervision, conceptualization, visualization, writing – original draft, validation, and funding acquisition. Pritam Kumar Roy: investigation, visualization, writing – original draft, and validation. Koichiro Uto: investigation, visualization, writing – original draft, and validation.

Conflicts of interest

There are no conflicts to declare.

Acknowledgements

References

1 T. G. Benton and W. A. Foster, *Proc. R. Soc. B*, 1992, **247**, 199–202.

2 P. Aussillous and D. Quéré, *Nature*, 2001, **411**, 924–927.

3 Y. Xue, H. Wang, Y. Zhao, L. Dai, L. Feng, X. Wang and T. Lin, *Adv. Mater.*, 2010, **22**, 4814–4818.

4 E. Bormashenko, *Langmuir*, 2017, **33**, 663–669.

5 L. Gao and T. J. McCarthy, *Langmuir*, 2007, **23**, 10445–10447.

6 V. Sivan, S.-Y. Tang, A. P. O'Mullane, P. Petersen, N. Eshtiaghi, K. Kalantar-zadeh and A. Mitchell, *Adv. Funct. Mater.*, 2013, **23**, 144–152.

7 D. Foresti, K. T. Kroll, R. Amissah, F. Sillani, K. A. Homan, D. Poulikakos and J. A. Lewis, *Sci. Adv.*, 2018, **4**, eaat1659.

8 D. Broboana, A.-M. Bratu, I. Magos, C. Patrascu and C. Balan, *Sci. Rep.*, 2022, **12**, 1774.

9 G. McHale and M. I. Newton, *Soft Matter*, 2011, **7**, 5473.

10 N. M. Oliveira, R. L. Reis and J. F. Mano, *Adv. Healthcare Mater.*, 2017, **6**, 1700192.

11 Y. Feng, G. Liu, J. Xu, K. Wang, W. Mao and G. Yao, *Langmuir*, 2022, **38**, 2055–2065.

12 Y. Feng, L. Wang, J. Xu and G. Liu, *Soft Matter*, 2022, **18**, 5230–5238.

13 M. Tenjimbayashi, S. Yamamoto and K. Uto, *Adv. Mater.*, 2023, **35**, 2300486.

14 J. Saczek, X. Yao, V. Zivkovic, M. Mamlouk, D. Wang, S. S. Pramana and S. Wang, *Adv. Funct. Mater.*, 2021, **31**, 2011198.

15 M. Tenjimbayashi and S. Fujii, *Small*, 2021, **17**, 2102438.

16 S. Fujii, S. Yusa and Y. Nakamura, *Adv. Funct. Mater.*, 2016, **26**, 7206–7223.

17 Y. Wang, K. Ma and J. H. Xin, *Adv. Funct. Mater.*, 2018, **28**, 1705128.

18 M. Tenjimbayashi, S. Samitsu and M. Naito, *Adv. Funct. Mater.*, 2019, **29**, 1900688.

19 E. Bormashenko, R. Balter and D. Aurbach, *J. Colloid Interface Sci.*, 2012, **384**, 157–161.

20 B. P. Binks and R. Murakami, *Nat. Mater.*, 2006, **5**, 865–869.

21 B. T. Lobel, C. A. Thomas, P. M. Ireland, E. J. Wanless and G. B. Webber, *Adv. Powder Technol.*, 2021, **32**, 1823–1832.

22 Y. Zhang, H. Cui, B. P. Binks and H. C. Shum, *Langmuir*, 2022, **38**, 9721–9740.

23 T. Onda, S. Shibuichi, N. Satoh and K. Tsujii, *Langmuir*, 1996, **12**, 2125–2127.

24 T. Sun, L. Feng, X. Gao and L. Jiang, *Acc. Chem. Res.*, 2005, **38**, 644–652.

25 P. Jin, K. Zhao, Z. Blin, M. Allais, T. Mouterde and D. Quéré, *J. Chem. Phys.*, 2023, **158**, 204709.

26 P. Aussillous and D. Quéré, *Proc. R. Soc. A*, 2006, **462**, 973–999.

27 G. McHale and M. I. Newton, *Soft Matter*, 2015, **11**, 2530–2546.

28 V. N. Paunov, *Langmuir*, 2003, **19**, 7970–7976.

29 N. Vogel, J. Ally, K. Bley, M. Kappl, K. Landfester and C. K. Weiss, *Nanoscale*, 2014, **6**, 6879–6885.

30 G. Gillies, M. Kappl and H.-J. Butt, *Adv. Colloid Interface Sci.*, 2005, **114**, 165–172.

31 D. Zang, Z. Chen, Y. Zhang, K. Lin, X. Geng and B. P. Binks, *Soft Matter*, 2013, **9**, 5067.

32 C. H. Ooi, C. Plackowski, A. V. Nguyen, R. K. Vadivelu, J. A. St. John, D. V. Dao and N.-T. Nguyen, *Sci. Rep.*, 2016, **6**, 21777.

33 T. Arbatan and W. Shen, *Langmuir*, 2011, **27**, 12923–12929.

34 E. Bormashenko, R. Pogreb, G. Whyman and A. Musin, *Colloids Surf., A*, 2009, **351**, 78–82.

35 E. Bormashenko, R. Pogreb, G. Whyman, A. Musin, Y. Bormashenko and Z. Barkay, *Langmuir*, 2009, **25**, 1893–1896.

36 U. Cengiz and H. Y. Erbil, *Soft Matter*, 2013, **9**, 8980.

37 X. Li, R. Wang, S. Huang, Y. Wang and H. Shi, *Soft Matter*, 2018, **14**, 9877–9884.

38 E. Bormashenko, A. Musin, G. Whyman, Z. Barkay, A. Starostin, V. Valtsifer and V. Strelnikov, *Colloids Surf., A*, 2013, **425**, 15–23.

39 R. Wang and X. Li, *Powder Technol.*, 2020, **367**, 608–615.

40 A. F. Stalder, T. Melchior, M. Müller, D. Sage, T. Blu and M. Unser, *Colloids Surf., A*, 2010, **364**, 72–81.

41 E. Bormashenko, *Curr. Opin. Colloid Interface Sci.*, 2011, **16**, 266–271.

42 F. Celestini and Ed. Bormashenko, *J. Colloid Interface Sci.*, 2018, **532**, 32–36.

43 Y. Asaumi, M. Rey, K. Oyama, N. Vogel, T. Hirai, Y. Nakamura and S. Fujii, *Langmuir*, 2020, **36**, 13274–13284.

44 R. Mayne, T. C. Draper, N. Phillips, J. G. H. Whiting, R. Weerasekera, C. Fullarton, B. P. J. de Lacy Costello and A. Adamatzky, *Langmuir*, 2019, **35**, 13182–13188.

45 T. H. Nguyen, K. Hapgood and W. Shen, *Chem. Eng. J.*, 2010, **162**, 396–405.

46 P. McEleney, G. M. Walker, I. A. Larmour and S. E. J. Bell, *Chem. Eng. J.*, 2009, **147**, 373–382.

47 Z. Liu, Y. Zhang, C. Chen, T. Yang, J. Wang, L. Guo, P. Liu and T. Kong, *Small*, 2018, 1804549.

48 B. T. Lobel, J. Fujiwara, S. Fujii, C. A. Thomas, P. M. Ireland, E. J. Wanless and G. B. Webber, *Mater. Adv.*, 2020, **1**, 3302–3313.

49 F. Geyer, Y. Asaumi, D. Vollmer, H. Butt, Y. Nakamura and S. Fujii, *Adv. Funct. Mater.*, 2019, **29**, 1808826.

50 M. Tenjimbayashi, Y. Watanabe, Y. Nakamura and M. Naito, *Adv. Mater. Interfaces*, 2020, **7**, 2000160.

51 D. Bartolo, F. Bouamrirene, É. Verneuil, A. Buguin, P. Silberzan and S. Moulinet, *Europhys. Lett.*, 2006, **74**, 299–305.

52 M. Reyssat, A. Pépin, F. Marty, Y. Chen and D. Quéré, *Europhys. Lett.*, 2006, **74**, 306–312.

53 K. Wang and W. Sun, *J. Eng. Mech.*, 2015, **143**, B4015004.

54 T. Mouterde, P. S. Raux, C. Clanet and D. Quéré, *Proc. Natl. Acad. Sci. U. S. A.*, 2019, **116**, 8220–8223.

55 D. Richard and D. Quéré, *Europhys. Lett.*, 1999, **48**, 286–291.

56 L. Mahadevan and Y. Pomeau, *Phys. Fluids*, 1999, **11**, 2449–2453.

57 J. Huang, Z. Wang, H. Shi and X. Li, *Soft Matter*, 2020, **16**, 4632–4639.

58 H. Y. Erbil, *Adv. Colloid Interface Sci.*, 2012, **170**, 67–86.

59 C. H. Ooi and N.-T. Nguyen, *Microfluid. Nanofluid.*, 2015, **19**, 483–495.

60 M. Dandan and H. Y. Erbil, *Langmuir*, 2009, **25**, 8362–8367.

61 G. McHale, N. J. Shirtcliffe, M. I. Newton, F. B. Pyatt and S. H. Doerr, *Appl. Phys. Lett.*, 2007, **90**, 054110.

62 A. Tosun and H. Y. Erbil, *Appl. Surf. Sci.*, 2009, **256**, 1278–1283.

63 C. H. Ooi, E. Bormashenko, A. V. Nguyen, G. M. Evans, D. V. Dao and N.-T. Nguyen, *Langmuir*, 2016, **32**, 6097–6104.

64 P. S. Bhosale, M. V. Panchagnula and H. A. Stretz, *Appl. Phys. Lett.*, 2008, **93**, 034109.

65 B. Laborie, F. Lachaussée, E. Lorenceau and F. Rouyer, *Soft Matter*, 2013, **9**, 4822.

66 A. Gallo, F. Tavares, R. Das and H. Mishra, *Soft Matter*, 2021, **17**, 7628–7644.

67 Y. Pan, K. Shi, X. Duan and G. F. Naterer, *Int. J. Heat Mass Transfer*, 2019, **129**, 953–964.

68 A. G. Marín, O. R. Enríquez, P. Brunet, P. Colinet and J. H. Snoeijer, *Phys. Rev. Lett.*, 2014, **113**, 054301.

69 Y. Zhao, C. Yang and P. Cheng, *Appl. Phys. Lett.*, 2021, **118**, 141602.

70 X. Zhang, X. Liu, J. Min and X. Wu, *Appl. Therm. Eng.*, 2019, **147**, 927–934.

71 A. Starostin, V. Strelnikov, L. A. Dombrovsky, S. Shoval and E. Bormashenko, *Colloids Surf., A*, 2022, **636**, 128125.

72 X. Lin, W. Ma, L. Chen, L. Huang, H. Wu and A. Takahara, *RSC Adv.*, 2019, **9**, 34465–34471.

73 P. K. Roy, I. Legchenkova, S. Shoval, L. A. Dombrovsky and E. Bormashenko, *J. Colloid Interface Sci.*, 2021, **592**, 167–173.

74 B. Wang, K. F. Chan, F. Ji, Q. Wang, P. W. Y. Chiu, Z. Guo and L. Zhang, *Adv. Sci.*, 2019, **6**, 1802033.

75 P. K. Roy, M. Frenkel, I. Legchenkova, S. Shoval, B. P. Binks and E. Bormashenko, *J. Phys. Chem. C*, 2020, **124**, 9345–9349.

76 P. K. Roy, S. Shoval, S. Fujii and E. Bormashenko, *J. Colloid Interface Sci.*, 2023, **630**, 685–694.

77 P. K. Roy, I. Legchenkova, S. Shoval and E. Bormashenko, *J. Phys. Chem. C*, 2021, **125**, 1414–1420.

78 E. Bormashenko, P. K. Roy, S. Shoval and I. Legchenkova, *Condens. Matter*, 2020, **5**, 62.

79 A. T. Tyowua and A. I. Ezekwuaku, *Colloids Surf., A*, 2021, **629**, 127386.

80 T. Braniste, V. Ciobanu, F. Schütt, H. Mimura, S. Raevschi, R. Adelung, N. M. Pugno and I. Tiginyanu, *Materials*, 2021, **14**, 5086.

81 E. Bormashenko, Y. Bormashenko, R. Grynyov, H. Aharoni, G. Whyman and B. P. Binks, *J. Phys. Chem. C*, 2015, **119**, 9910–9915.

82 M. J. Kreder, J. Alvarenga, P. Kim and J. Aizenberg, *Nat. Rev. Mater.*, 2016, **1**, 15003.

83 M. Tenjimbayashi and K. Manabe, *Sci. Technol. Adv. Mater.*, 2022, **23**, 473–497.

84 H. Saini, P. Kallem, E. Otyepková, F. Geyer, A. Schneemann, V. Ranc, F. Banat, R. Zbořil, M. Otyepka, R. A. Fischer and K. Jayaramulu, *J. Mater. Chem. A*, 2021, **9**, 23651–23659.

85 P. M. Ireland, C. A. Thomas, B. T. Lobel, G. B. Webber, S. Fujii and E. J. Wanless, *J. Phys.: Conf. Ser.*, 2019, **1322**, 012006.

86 C. P. Whitby, X. Bian and R. Sedev, *Soft Matter*, 2012, **8**, 11336.

87 M. Tenjimbayashi, *Appl. Phys. Lett.*, 2023, **122**, 251604.

88 B. S. Lekshmi and S. N. Varanakkottu, *Langmuir*, 2022, **38**, 11743–11752.

89 B. S. Lekshmi, A. S. Yadav, P. Ranganathan and S. N. Varanakkottu, *Langmuir*, 2020, **36**, 15396–15402.

90 P. K. Roy, B. P. Binks, S. Shoval, L. A. Dombrovsky and E. Bormashenko, *Colloids Surf., A*, 2022, **649**, 129453.

91 Y.-E. Miao, H. K. Lee, W. S. Chew, I. Y. Phang, T. Liu and X. Y. Ling, *Chem. Commun.*, 2014, **50**, 5923–5926.

92 V. Lotito and T. Zambelli, *Adv. Colloid Interface Sci.*, 2022, **299**, 102538.

93 U. Ulusoy, *Minerals*, 2023, **13**, 91.

94 J. Fujiwara, F. Geyer, H. Butt, T. Hirai, Y. Nakamura and S. Fujii, *Adv. Mater. Interfaces*, 2020, **7**, 2001573.

95 B. P. Binks, S. K. Johnston, T. Sekine and A. T. Tyowua, *ACS Appl. Mater. Interfaces*, 2015, **7**, 14328–14337.

96 W. Wang, C. L. Bray, D. J. Adams and A. I. Cooper, *J. Am. Chem. Soc.*, 2008, **130**, 11608–11609.

97 Z. Zhao, C. Ling, D. Wang, J. Wang, J. Saczek, S. Pramana, S. Sridhar, J. Shang, B. B. Xu, D. C. W. Tsang, J. Chen and S. Wang, *Small*, 2020, **16**, 2002802.

98 H. Zhao, Y. Yang, Y. Chen, J. Li, L. Wang and C. Li, *Chem. Eng. Sci.*, 2022, **248**, 117085.

99 P. K. Roy, B. P. Binks, E. Bormashenko, I. Legchenkova, S. Fujii and S. Shoval, *J. Colloid Interface Sci.*, 2020, **575**, 35–41.

100 D. Quéré, *Rep. Prog. Phys.*, 2005, **68**, 2495–2532.

101 T.-S. Wong, S. H. Kang, S. K. Y. Tang, E. J. Smythe, B. D. Hatton, A. Grinthal and J. Aizenberg, *Nature*, 2011, **477**, 443–447.

102 A. Lafuma and D. Quéré, *Europhys. Lett.*, 2011, **96**, 56001.

103 M. Anyfantakis, V. S. R. Jampani, R. Kizhakidathazhath, B. P. Binks and J. P. F. Lagerwall, *Angew. Chem., Int. Ed.*, 2020, **59**, 19260–19267.

104 P. K. Roy, B. P. Binks, S. Shoval, L. A. Dombrovsky and E. Bormashenko, *J. Colloid Interface Sci.*, 2022, **626**, 466–474.

105 K. Aono, K. Ueno, S. Hamasaki, Y. Sakurai, S. Yusa, Y. Nakamura and S. Fujii, *Langmuir*, 2022, **38**, 7603–7610.

106 T. Takei, R. Tomimatsu, T. Matsumoto, K. R. Sreejith, N.-T. Nguyen and M. Yoshida, *Polymers*, 2022, **14**, 4849.

107 R. Murakami, S. Kobayashi, M. Okazaki, A. Bismarck and M. Yamamoto, *Front. Chem.*, 2018, **6**, 435.

108 R. W. Style, R. Boltyanskiy, Y. Che, J. S. Wettlaufer, L. A. Wilen and E. R. Dufresne, *Phys. Rev. Lett.*, 2013, **110**, 066103.

109 B. Andreotti and J. H. Snoeijer, *Annu. Rev. Fluid Mech.*, 2020, **52**, 285–308.

110 M. Tenjimbayashi, S. Samitsu, Y. Watanabe, Y. Nakamura and M. Naito, *Adv. Funct. Mater.*, 2021, **31**, 2010957.

111 C. P. McLaren, T. M. Kovar, A. Penn, C. R. Müller and C. M. Boyce, *Proc. Natl. Acad. Sci. U. S. A.*, 2019, **116**, 9263–9268.

112 B. S. Lekshmi and S. N. Varanakkottu, *Droplet*, 2023, **2**, e44.

113 J. Fujiwara, A. Yokoyama, M. Seike, N. Vogel, M. Rey, K. Oyama, T. Hirai, Y. Nakamura and S. Fujii, *Mater. Adv.*, 2021, **2**, 4604–4609.

114 J. Niu, W. Liu, J. X. Li, X. Pang, Y. Liu, C. Zhang, K. Yue, Y. Zhou, F. Xu, X. Li and F. Li, *Nat. Commun.*, 2023, **14**, 3853.

115 C. Py, P. Reverdy, L. Doppler, J. Bico, B. Roman and C. N. Baroud, *Phys. Rev. Lett.*, 2007, **98**, 156103.

116 Y. Zhang, Z. Huang, Z. Cai, Y. Ye, Z. Li, F. Qin, J. Xiao, D. Zhang, Q. Guo, Y. Song and J. Yang, *Sci. Adv.*, 2021, **7**, eabi7498.

117 X. Li, Y. Xue, P. Lv, H. Lin, F. Du, Y. Hu, J. Shen and H. Duan, *Soft Matter*, 2016, **12**, 1655–1662.

118 X. Guo, N. Xue, M. Zhang, R. Ettelaie and H. Yang, *Nat. Commun.*, 2022, **13**, 5935.

119 Z. Wang, G. Zhu, Q. Wang, K. Ding, Y. Tong and C. Gao, *Sep. Purif. Technol.*, 2022, **301**, 122046.

120 S. Wooh, H. Huesmann, M. N. Tahir, M. Paven, K. Wichmann, D. Vollmer, W. Tremel, P. Papadopoulos and H.-J. Butt, *Adv. Mater.*, 2015, **27**, 7338–7343.

121 J. Heo, J. Lee, W. Shim, H. Kim, S. Fujii, J. Lim, M. Kappl, H.-J. Butt and S. Wooh, *ACS Appl. Mater. Interfaces*, 2023, **15**, 38986–38995.

122 H. Tan, S. Wooh, H.-J. Butt, X. Zhang and D. Lohse, *Nat. Commun.*, 2019, **10**, 478.

123 S. M. Salehabad and S. Azizian, *Colloids Surf., A*, 2021, **620**, 126551.

124 Y. Kim, S. Oh, H. Lee, D. Lee, M. Kim, H. S. Baek, W. S. Park, E. Kim and J.-H. Jang, *Biomater. Sci.*, 2021, **9**, 1639–1651.

125 S. M. Salehabad, S. Azizian and S. Fujii, *Langmuir*, 2019, **35**, 8950–8960.

126 V. Narayanamurthy, Z. E. Jeroish, K. S. Bhuvaneshwari, P. Bayat, R. Premkumar, F. Samsuri and M. M. Yusoff, *RSC Adv.*, 2020, **10**, 11652–11680.

127 D. T. Tran, A. S. Yadav, N.-K. Nguyen, P. Singha, C. H. Ooi and N.-T. Nguyen, *Small*, 2023, 2303435.

128 Z. Huang, Y. Xie, H. Chen, Z. Yu, L. Shi and J. Jin, *Processes*, 2023, **11**, 983.

129 N.-K. Nguyen, C. H. Ooi, P. Singha, J. Jin, K. R. Sreejith, H.-P. Phan and N.-T. Nguyen, *Processes*, 2020, **8**, 793.

130 E. Bormashenko, R. Balter and D. Aurbach, *Int. J. Chem. React. Eng.*, 2011, **9**, 1.

131 W. Wei, R. Lu, W. Ye, J. Sun, Y. Zhu, J. Luo and X. Liu, *Langmuir*, 2016, **32**, 1707–1715.

132 K. Lin, R. Chen, L. Zhang, D. Zang, X. Geng and W. Shen, *ACS Appl. Mater. Interfaces*, 2019, **11**, 8789–8796.

133 J. Tian, T. Arbatan, X. Li and W. Shen, *Chem. Commun.*, 2010, **46**, 4734.

134 A. Adamatzky, M. Tsompanas, T. C. Draper, C. Fullarton and R. Mayne, *ChemPhysChem*, 2020, **21**, 90–98.

135 N. El-Atab, R. B. Mishra, F. Al-Modaf, L. Joharji, A. A. Alsharif, H. Alamoudi, M. Diaz, N. Qaiser and M. M. Hussain, *Adv. Intell. Syst.*, 2020, **2**, 2000128.

136 C. H. Ooi, R. Vadivelu, J. Jin, K. R. Sreejith, P. Singha, N.-K. Nguyen and N.-T. Nguyen, *Lab Chip*, 2021, **21**, 1199–1216.

137 Y. Sun, Y. Zheng, C. Liu, Y. Zhang, S. Wen, L. Song and M. Zhao, *RSC Adv.*, 2022, **12**, 15296–15315.

138 N.-K. Nguyen, P. Singha, Y. Dai, K. R. Sreejith, D. T. Tran, H.-P. Phan, N.-T. Nguyen and C. H. Ooi, *Lab Chip*, 2022, **22**, 1508–1518.

139 X. Pang, M. Duan, H. Liu, Y. Xi, H. Shi and X. Li, *ACS Appl. Mater. Interfaces*, 2022, **14**, 11999–12009.

140 N. Barman, A. Shome, S. Kumar, P. Mondal, K. Jain, M. Tenjimbayashi and U. Manna, *Adv. Funct. Mater.*, 2023, **33**, 2214840.

141 T. C. Draper, N. Phillips, R. Weerasekera, R. Mayne, C. Fullarton, B. P. J. de Lacy Costello and A. Adamatzky, *Lab Chip*, 2020, **20**, 136–146.

142 J. C. Gomez, N. S. Vishnosky, S. T. Kim, S. A. Dinca, E. B. Finkelstein and R. C. Steinhardt, *Adv. Funct. Mater.*, 2023, **33**, 2214893.

143 S. X. Leong, L. K. Koh, C. S. L. Koh, G. C. Phan-Quang, H. K. Lee and X. Y. Ling, *ACS Appl. Mater. Interfaces*, 2020, **12**, 33421–33427.

144 H. Li, P. Liu, R. Gunawan, Z. M. Simeneh, C. Liang, X. Yao and M. Yang, *Adv. Healthcare Mater.*, 2021, **10**, 2001658.

145 J. Niu, H. Shi, H. Wei, B. Gao, J. X. Li, F. Xu, X. Li and F. Li, *Anal. Chem.*, 2020, **92**, 9048–9056.

146 M. Liu, C. Chen, J. Yu, H. Zhang, L. Liang, B. Guo, Y. Qiu, F. Yao, H. Zhang and J. Li, *Mater. Today Bio*, 2022, **17**, 100477.

147 A. Langella, S. D. Gadau, E. Serra, D. Bebbere and S. Ledda, *Biology*, 2022, **11**, 492.

148 R. Vadivelu, N. Kashaninejad, M. R. Nikmaneshi, R. R. Khadim, S. S. Salehi, N. C. Ramulu, Y. Sakai, M. Nishikawa, B. Firoozabadi and N. Nguyen, *Adv. Biol.*, 2021, **5**, 2000108.

149 W. Ramadhan, Y. Ohama, K. Minamihata, K. Moriyama, R. Wakabayashi, M. Goto and N. Kamiya, *J. Biosci. Bioeng.*, 2020, **130**, 416–423.

150 J. Aalders, L. Léger, T. Tuerlings, S. Ledda and J. van Hengel, *MethodsX*, 2020, **7**, 101065.

151 A. Walther, *Adv. Mater.*, 2020, **32**, 1905111.

152 T. Matsuda, R. Kawakami, R. Namba, T. Nakajima and J. P. Gong, *Science*, 2019, **363**, 504–508.

153 Y. Wang, L. Li, D. Hofmann, J. E. Andrade and C. Daraio, *Nature*, 2021, **596**, 238–243.

154 M. Tenjimbayashi and M. Naito, *Adv. Funct. Mater.*, 2022, **32**, 2204681.

155 J. Zhang, B. Chen, X. Chen and X. Hou, *Adv. Mater.*, 2021, **33**, 2005664.